Post-Compression of 9.2-μm Terawatt Laser Pulses to Femtoseconds

Igor V. Pogorelsky*, *Mikhail N.* Polyanskiy, *Marcus* Babzien and *Mark A.* Palmer

Accelerator Test Facility, Brookhaven National Laboratory, Upton, NY 11973, USA

Abstract. Contemporary CO_2 laser systems are capable to delivering picosecond pulses of the multi-terawatt peak power. Further pulse compression to a few cycles is possible using a post-compression in bulk materials with negative group velocity dispersion (GVD). We have experimentally demonstrated the post-compression of a long-wave infrared (9.2 μm) 150-GW peak power pulse from 1.85 ps to less than 500 fs using a combination of two optical materials with significantly different ratios of the nonlinear refractive index to the GVD coefficient. Such combination allows for optimization of the compression mechanism and promises a viable path to scaling peak powers to multi-terawatt levels.

1 Introduction

Recent years have seen a growing interest in applying long-wave infrared (LWIR) lasers (λ>4 μm) to strong-field physics research. This comes as the realization of benefits from the wavelength scaling for such applications as electron acceleration in plasma wake fields, ion beam generation from gas jets, intense gamma sources via inverse Compton scattering, energy transport through air, HHG, etc. The extension of experimental studies of these and other phenomena into the LWIR spectral domain can be enabled by CO_2 lasers capable to producing picosecond pulses at λ≈10 μm and several joule energies [1, 2]. However, the continuing advancement of ultra-fast laser applications calls for down to few optical cycles, sub-picosecond LWIR pulses at the multi-terawatt peak power.

The duration of an ultra-short laser pulse is limited by the spectral bandwidth of the laser gain, which does not exceed ~1 THz for a CO_2 laser potentially allowing to attain 500 fs [3]. However, the present-day CO_2 laser systems are restricted to a few-picosecond minimum pulse duration due to the spectral narrowing of ultra-short seed pulses under a high amplification.

Sub-picosecond post-compression of picosecond pulses at the several terawatt peak power can be explored through their self-phase modulation (SPM) $\Delta\phi(t) = -\left(\frac{\omega_0}{c}\right) n_2 I(t) L_1$ on their propagation through an optical material of the thickness L_1 with the nonlinear refraction index n_2, where I is the laser intensity, ω_0 is the laser central frequency and c is the speed of light. This phase shift results in the frequency chirp $\Delta\omega(t) = \frac{d(\Delta\phi)}{dt} = -\left(\frac{\omega_0}{c}\right) n_2 L_1 \frac{dI}{dt}$. Followed by dispersive compression with diffraction gratings, a chirped mirror, or a bulk material of a length L_2 with a negative group velocity dispersion (GVD) this phase chirp can be compensated resulting in a pulse compression by $\Delta t \approx \Delta\omega(GVD)L_2$. This idea has been explored theoretically and experimentally mainly for the purpose of improving characteristics of near-IR solid state lasers [4, 5]. Some recent works address also LWIR lasers at λ≈4 μm [6] and λ≈10 μm with NaCl as the material for both SPM and GVD [7-9]. However, until now, this technique was never experimentally verified with CO_2 lasers.

We report here the first experimental demonstration on post-compression of 2-ps, terawatt-class CO_2 laser pulses to sub picoseconds using optical materials transparent at the λ=9.2 μm.

2 Experiment

We used in our experiment a 5-TW, 1.85-ps CO_2 CPA laser system operated at the BNL/ATF [2]. The central wavelength of this laser filled with a multi-atmosphere mixture of $C^{16,18}O_2$ isotopes is 9.2 μm. The experimental setup for a proof-of-principle demonstration of the post-compression is shown in Fig. 1.

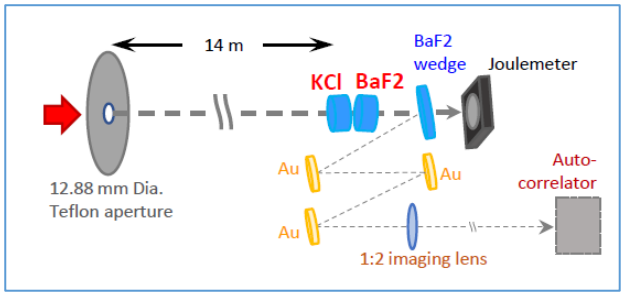

Fig. 1. Experimental setup for studying the post-compression.

A close to Gaussian beam of up to 500 mJ energy is produced in this scheme by sending the output beam from

* Corresponding author: igor@bnl.gov

a several-Joule laser amplifier of the 10 cm optical aperture through a 13 mm diameter Teflon aperture. The intensity distribution after 14 m of propagation is defined by far-field diffraction and practically does not depend on the profile of the input beam. The KCl and BaF_2 50 mm thick slabs were chosen for a SPM chirper and a GVD compressor, correspondingly, based on their n_2 and GVD characteristics shown in Table 1. Among the shown three materials, KCl has the highest absolute $n_2/(GVD)$ ratio, exceeding that of NaCl by roughly a factor of two and BaF_2 by more than a factor of eight. This led to the choice of KCl for the first element of the compressor, which is primarily responsible for the SPM part of the process, and BaF_2 for the downstream element, which provides the dispersive compensation of the chirp.

Table 1. Material properties at 9.2 μm.

	n_0	(GVD) (fs²/mm)	n_2 (m²/W)
NaCl	1.500	-1010	3.5×10^{-20}
KCl	1.459	-558	3.4×10^{-20}
BaF_2	1.412	-2340	1.7×10^{-20}

A BaF_2 lens was used for imaging the output surface of the BaF_2 slab on the 10×10 mm crystal of a single-shot autocorrelator (AC) with the ×2 optical magnification. Representative AC traces recorded at different laser energies are shown in Fig. 2 together with their horizontal intensity projections. Compression to sub-picosecond duration is observed for all pulses with input energies exceeding 200 mJ. The highest peak intensity is achieved at the 275 mJ joulemeter readout corresponding to ~450 mJ/cm² incident laser peak fluence. At higher energies, the AC signal gradually decreases due to nonlinear absorption in KCl and BaF_2 despite the continued shortening of the pulse.

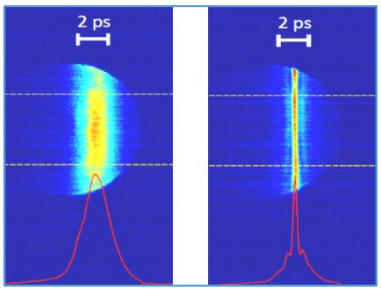

Fig. 2. AC images obtained at the 450 mJ/cm² incident laser peak fluence without post-compression (left) and with a two-element KCl+BaF_2 compressor (right).

Spectrum evolution has been recorded in a similar setup with a single-shot spectrometer of the 8 nm wavelength resolution installed in the position of the imaging lens in Fig. 1. Spectra of a pulse before and after the post-compression are shown in Fig. 3. The broadened spectrum is for the laser pulse with the energy matching the conditions of the optimal post-compression. The fine structure of the spectra is due to the rotational modulation of the gain spectrum of CO_2 laser amplifiers.

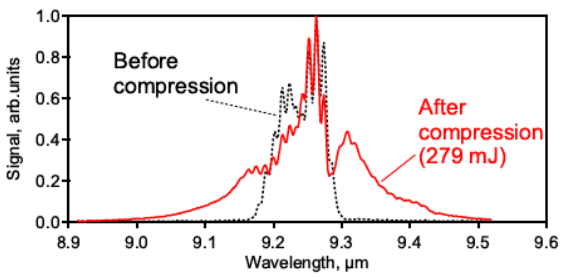

Fig. 3. A typical measured spectra of a laser pulse before and after compression at the energy corresponding to the optimal compression.

3 Discussions and prospects

The numerical modeling of the post-compression is done with the *co2amp* software [10]. For input parameters, it uses the results of a comprehensive modeling of a chirped-pulse amplification of a picosecond LWIR pulse in a chain of high-pressure, mixed-isotope CO_2 laser amplifiers followed by the propagation in air. A split-step algorithm is used for modeling the interaction of the laser pulse with the compressor materials. To compare the model predictions with experimental AC curves, we first model the dynamics of the pulse compression in the central portion of the beam of the 5 mm diameter as is seen by the AC chip. We have found that the model accurately reproduces experimental AC curves in a wide range of the laser pulse energies, including the optimal post-compression regime. The simulated output spectrum agrees reasonably well with the spectrum measured experimentally, yet again confirming the accuracy of the model.

The results of the pulse modeling at different stages of the post-compression (the input, after the first element, and at the output of the post-compressor) are shown in Fig. 4 by dotted black, solid blue, and solid red lines, respectively. The left portion of Fig. 4 corresponds to the 5 mm diameter central portion of the beam. Here, the output pulse profile agrees to a high accuracy with the deconvolution of the AC trace shown in Fig. 2 (right).

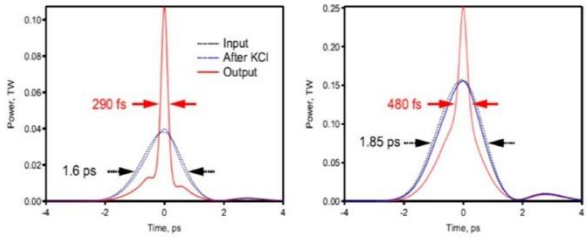

Fig. 4. Results of numerical modelling of the pulse compression in the KCl+BaF_2 configuration at the conditions corresponding to the optimum compression; left – input and output temporal profiles integrated over the 5 mm diameter central portion of a laser beam seen by the AC crystal; right – the same but integrated over the entire beam.

Note that the duration of the input pulse is shorter in the beam center than in the outer areas of the beam: 1.6 ps (FWHM) in the center vs. 1.85 ps beam-average. This is due to a pulse compression in air that occurs by the same manner as the compression in bulk solids (SPM

accompanied by negative GVD) but requires longer propagation due to orders-of-magnitude smaller n_2 and dispersion.

The simulated temporal profiles agree with deconvoluted experimental AC traces. This allows us to conclude that we achieved a post-compression of a 1.6-ps pulse to <300 fs in the center of a near-Gaussian beam with a 180% increase of the peak intensity.

At the same time, the simulations allow us to gain the understanding of the pulse evolution averaged over the entire beam. Figure 4 (right) shows that the entire 1.85-ps pulse gets compressed to 500 fs with the 60% of the power increase.

Our initial demonstration of delivering hundreds of millijoule on the femtosecond time scale surpass by far the results previously achieved in the LWIR spectral domain. The implemented here partial decoupling between the SPM spectral stretching and GVD pulse compression by using a combination of two materials with contrasting $n_2/(GVD)$ ratios allows matching the nonlinear spectrum broadening with the GVD phase delay compensation while keeping B-integral on each optical slab below the threshold for parasitic micro-filamentation and nonlinear absorption (B≤3).

Experiments will continue towards further improving the efficiency of the LWIR energy conversion to femtoseconds by optimizing the post-compressor staging. We expect that our continuing material search and optimization of the beam and the setup geometry will lead to a practical system for an effective femtosecond conversion of the entire CO_2 laser output at a multi-terawatt level as is required for advanced plasma accelerators and other strong-physics research and applications.

Acknowledgements

This research is funded by the US Department of Energy (DOE) Accelerator Stewardship Program grant, B& R #KA2601020. BNL Laboratory Directed Research and Development (LDRD) grant #20-010 AD/NPP.

References

1. D. Haberberger, S. Tochitsky and C. Joshi, "Opt. Express, **18**, 17865 (2010)
2. M. P. Polyanskiy, I. V. Pogorelsky, M. Babzien and M. A. Palmer, OSA Continuum, **3**, 459 (2020)
3. M. P. Polyanskiy, I. V. Pogorelsky, M. Babzien, R. Kupfer, N. Vafaei-Najafabadi and M. A. Palmer, Photonics, **8**, 101 (2021)
4. A. A. Voronin, A. M. Zheltikov, T. Ditmire, B. Rus and G. Korn, Opt. Commun., **291**, 299 (2013)
5. S. Hädrich, et al, Opt. Lett., **41**, 4332 (2016)
6. M. Hemmer, M. Baudisch, A. Thai, A. Couairon and J. Biegert, Opt. Express, **21**, 28095 (2013)
7. B. G. Bravy, V. M. Gordienko and V. T. Platonenko, Laser Phys. Lett., **11**, 065401 (2014)
8. J. Pigeon, S. Tochitsky and C. Joshi, AIP Conf. Proc., **1777**, 110005 (2016)
9. B. G. Bravy, V. M. Gordienko and V. T. Platonenko, J. of Russ. Laser Research, **37**, 465 (2016)
10. M. N. Polyanskiy, Appl. Opt. **54**, 5136 (2015)